Computer Modeling Study on the Phase Morphology of PS-*b*-PMMA Copolymers

Dan Mu,[1] Jian-Quan Li,[2] Song Wang[3]

[1]*Department of Chemistry, Zaozhuang University, Shandong 277160, China*
[2]*Department of Physics and Electronic Engineering, Zaozhuang University, Shandong 277160, China*
[3]*State Key Laboratory of Theoretical and Computational Chemistry, Institute of Theoretical Chemistry, Jilin University, Changchun 130023, China*

Received 21 November 2009; accepted 28 March 2010
DOI 10.1002/app.32538
Published online 21 July 2010 in Wiley Online Library (wileyonlinelibrary.com).

ABSTRACT: The phase morphologies of six kinds of designed poly(styrene-*block*-methyl methacrylate) copolymers were studied at 383, 413, and 443 K by mesoscopic modeling. The values of order parameter depended on both the structures of block copolymers and the simulation temperatures, whereas values of order parameter of the long chains were higher than those of the short ones; temperature showed a more obvious effect on long chains than on the short ones. These plain copolymers doped with PS or PMMA homopolymer showed different order parameter values. When the triblock copolymer was composed of the same component at both ends and was doped with a homopolymer with the same component as that in the middle of triblock copolymer, such as B6A3B6 doped with A3, B12A6B12 doped with A6, A6B12A6 doped with B12, and A3B6A3 doped with B6, it showed the highest order parameter values. The study of copolymers doped with nanoparticles showed that the mesoscopic phase was influenced by not only the properties of the nanoparticles, such as the size and density, but also the compositions of copolymers. © 2010 Wiley Periodicals, Inc. J Appl Polym Sci 119: 265–274, 2011

Key words: blending; block copolymers; calculations

INTRODUCTION

The spontaneous formation of nanostructured materials by molecular self-assembly of block copolymers is an active area of research driven both by its inherent beauty and by a wealth of potential technological applications. Thin films of self-organizing diblock copolymers may be suitable for semiconductor applications as they enable patterning of ordered domains with dimensions below photolithographic resolution over wafer-scale areas.[1] Block copolymers are known to generate nanoscale microdomains by microphase separation if they are annealed at a temperature lower than their order-disorder transition temperatures.[2] Block copolymer thin films with well defined nanostructures have recently received considerable attention for their potential nanofabrication applications.[3–10] In these applications, controlling the morphology of the block copolymer thin film, particularly the orientation and order of the phase-separated microdomain, is essential.

Polystyrene (PS) and poly(methyl methacrylate) (PMMA) are classic model systems in polymer science and they have similar glass transition temperatures. PS/PMMA blends are a type of well-known immiscible combination,[11–18] and their bulk and surface phase separation has been observed.[19,20] Immiscible blends are known to have properties combining those of both the polymers and also to have segregated structures with domains predominantly formed from the individual homopolymers. It has been shown that changing the relative homopolymer proportions in such blends can vary the domain structure, surface morphology, even the phase morphology.[21–23] However, there have been no reports about the inducing effects of nanoparticles on a polystyrene-*block*-poly(methyl methacrylate) (PS-*b*-PMMA) system, whose plain blends are immiscible. Some inspiring results were obtained in this work, which can be applied to nanofabrication to improve the function of nanomaterials.

SIMULATION DETAILS, RESULTS, AND DISCUSSION

Mesoscale structures are of utmost importance during the production processes of many materials, such as polymer blends, block copolymer systems, surfactant aggregates in detergent materials, latex particles, and drug delivery systems. Mesoscopic dynamics models are receiving increasing attention as they form a bridge between studies of microscale and macroscale properties.[24–27] Our simulation

Correspondence to: D. Mu (mudanjlu1980@yahoo.com.cn).

processes were all carried out with the MesoDyn package in the Materials Studio commercial program provided by Accerlys Company on an SGI workstation. MesoDyn deals with the dynamic mean-field density functional theory (DFT) in which the dynamics of phase separation can be described by Langevin-type equations to investigate polymer diffusion. The thermodynamic forces are found via mean-field DFT, taking the Gaussian chain as a model. The coarse-grained Gaussian chain consists of beads of equal length and equal volume. When the free energy of the system remains stable with increasing simulation time, the phase separation becomes complete. In the study on the compatibility of PEO/PMMA blends in our former work, the MesoDyn simulation method was also selected to detect the phase morphologies of PEO/PMMA blends. The calculation results obtained from that study clarified several conflicting conclusions from different experiments from a theoretical point of view.[28]

The order parameter, denoted as P, is defined as the average volume of the difference between the local density squared and the overall density squared, given by the equation

$$P_i = \frac{1}{V}\int_V [\eta_i^2(r) - \eta_i^2]dr,$$

where ν_i is dimensionless density (volume fraction) for species i. The larger the value of P data is the stronger the phase separation is. A decrease in P indicates better compatibility or miscibility and the polymer phases mix more randomly.

This article consists of two parts: (1) design of six kinds of PS-*b*-PMMA copolymers with different chain lengths and arrangement types to study their compatibility and study of the temperature effect on the compatibility of PS-*b*-PMMA, and (2) on the basis of the first part, design of seven kinds of nanoparticles arrangements to study their inducing effects on phase morphologies.

The study on the compatibility of plain PS-*b*-PMMA

Model

To study the compatibility of different PS-*b*-PMMA copolymers, six types of copolymers denoted as A3B6, A6B12, A3B6A3, A6B12A6, B6A3B6, and B12A6B12 were designed, in which A and B represent PS and PMMA segments, respectively. For convenience, A3B6 and A6B12 were defined as the "AB" groups; A3B6A3 and A6B12A6 were defined as the "ABA" group; B6A3B6 and B12A6B12 were defined as the "BAB" group. The former of each group represents short PS-*b*-PMMA chains and the latter represents long ones; the chain length of the latter was twice as long as the former in the same group.

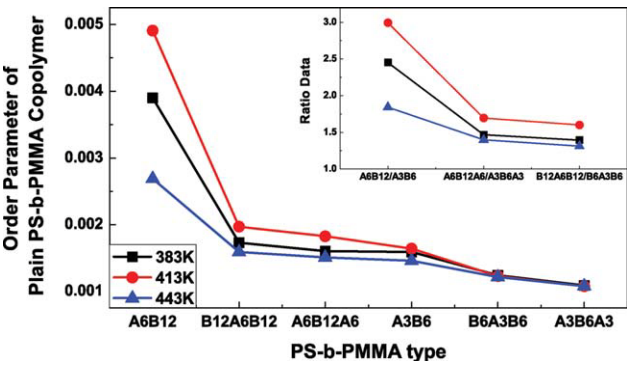

Figure 1 The P values of six types of PS-*b*-PMMA copolymer under different temperatures. [Color figure can be viewed in the online issue, which is available at

Results and discussion

Several features can be seen in Figure 1:

(1) The T_g values of PMMA and PS are both around 370 K, and the simulation temperature were 383, 413, and 443 K, which were all higher than T_g of PEO and PMMA. Therefore, the block copolymers we designed would move freely under simulation temperatures. The P values of long chains (A6B12, B12A6B12, and A6B12A6) were all higher than those of the short ones (A3B6, B6A3B6, and A3B6A3), respectively, which means the long PS-*b*-PMMA copolymers were more likely to undergo microscopic phase separation. From the order of P values: $P_{A6B12} > P_{A3B6}$, $P_{B12A6B12} > P_{B6A3B6}$, and $P_{A6B12A6} > P_{A3B6A3}$, it can be derived that for long chains, when their "A" and "B" segments were both long enough, microscopic areas consisting of the same component would appear and even microscopic separation could occur.

(2) For both the long chained and short-chained PS-*b*-PMMA copolymers, the order of P values was the same, which was $P_{\text{"AB"}} > P_{\text{"BAB"}} > P_{\text{"ABA"}}$. It resulted from both the difference in diffusion coefficient between PS and PMMA,[29] and the difference in the copolymer-type. The diffusion coefficient of PS is smaller than PMMA, so the copolymer rich in PS component, such as those in the "ABA" group, presented a smaller P value because more PS would retard the movement of the whole chain. For "AB" and "BAB" groups, they had the same amount of PS, but were different in

copolymer-type. The "AB" group was actually simpler and more heterogenous compared with the "BAB" group, so phase separation was more likely to occur in the "AB" group under the same condition.

(3) For both long- and short-chained copolymers, the P values of the "AB" group were higher than those of the "BAB" and "ABA" groups at 383, 413, and 443 K, respectively. Furthermore, the order of temperature effect on order parameter was the same, that is, $P_{413K} > P_{383K} > P_{443K}$, and the differences in order parameter values under different temperatures of "AB" group were obviously higher than those of the other two groups. These resulted from the most efficient heterogeneity of the "AB" group compared with the other two groups. Temperature had a bigger effect on the long chains than on the short chains because of the difference in the diffusion coefficient of PS and PMMA. The longer the chain, the slower it moves to adjust its configuration to form stable phase morphology.

(4) The inserted figure shows the ratios of P values (defined as R values) of each group under three temperatures. To describe these R values clearly, the "AB" group is taken as an example. The quotient of P value of A6B12 divided by the P value of A3B6 equals to the R value. The order of R values was the same at 383, 413, and 443 K, which was $R_{"AB"} > R_{"ABA"} > R_{"BAB"}$. From R values of the copolymers obtained based on their corresponding short chains, it can be seen that the effect of increase in chain length on P values for the "AB" group was the most obvious, whereas those for the "ABA" and "BAB" groups were similar. The main reason is that of the "AB" group with "A" and "B" lying on two ends could achieve the highest degree of heterogeneity compared with the "ABA" and "BAB" groups. The "ABA" and "BAB" groups both showed a certain degree of heterogeneity, but the components of both ends were the same, which could reduce the degree of heterogeneity. Taking the "ABA" group as an example, it can be seen that both ends were the same "A" component, which could shield the "B" segment, resulting in a situation similar to that with the pure "A" component. Accordingly, the "BAB" group showed a situation similar to that of pure PMMA with only the "B" component. Therefore, the effect of an increase in the chain length on P values for the "ABA" and "BAB" groups was not obvious compared with that for the "AB" group. From the differences among P values at different temperatures, it can be seen that the "AB" group showed more sensitive to the change of temperature than the other two groups.

PS-*b*-PMMA copolymer doped with either of its own components

Model

The models of this part can be divided into two types according to which component, PS or PMMA, was doped into the PS-*b*-PMMA copolymer. The chain length of the dopant homopolymer was the same as that of its counterpart in the PS-*b*-PMMA copolymer. The models are listed as follows.

The first type consisted of six models doped with component A; they were A3B6 doped with A3, A6B12 doped with A6, A3B6A3 doped with A3, A6B12A6 doped with A6, B6A3B6 doped with A3, and B12A6B12 doped with A6. The second type, which had the same number as the first type, were copolymers doped with component B. They were A3B6 doped with B6, A6B12 doped with B12, A3B6A3 doped with B6, A6B12A6 doped with B12, B6A3B6 doped with B6, and B12A6B12 doped with B12.

Results and discussion

Subfigures a1 and a2 in Figure 2 show the P values of two types of models, respectively. Subfigures b1 and b2 show their corresponding R values based on the pure PS-*b*-PMMA copolymer with R values showing the effect of dopants on P values. The data of X-axis are the weight percentages of PS-*b*-PMMA copolymer; weight percentages of 18, 33, 55, and 67% were chosen as examples. Some features can be seen in Figure 2:

(1) Subfigure a1 is similar to subfigure b1, and subfigure a2 is also similar to subfigure b2, which means the doping effects of both PS and PMMA were nearly in direct proportion to the amount of dopants compared with pure PS-*b*-PMMA copolymer.

(2) The R values here are defined as the quotients of P values of the copolymers with homopolymer dopants divided by the P value of pure PS-*b*-PMMA. A reference line is drawn through the R value of 1 in subfigures b1 and b2; when an R value lies above the line, the doping effect is considered a reinforcing effect; otherwise, the doping effect is considered a weakening effect. The R values of 18% PS-*b*-PMMA copolymer doped with both PS and PMMA in subfigures b1 and b2 are all below the reference line except the case doped with

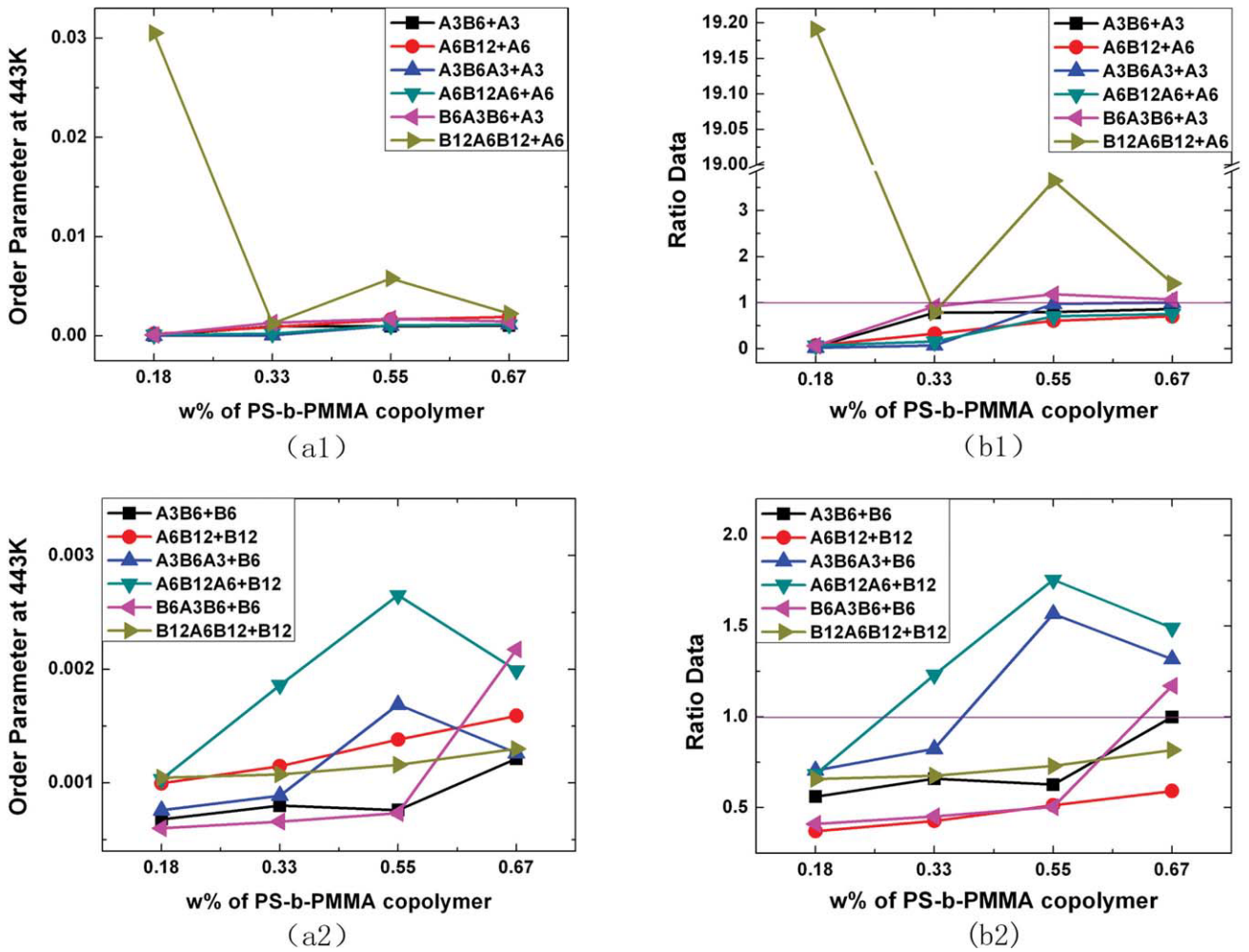

Figure 2 The *P* and *R* value of two kinds of PS-*b*-PMMA copolymers doped with its constructing components at 443 K, respectively. [Color figure can be viewed in the online issue, which is available at wileyonlinelibrary.com.]

A6, which means in most cases a weakening effect occurred with this 18% copolymer. Because there was only a small amount of PS-*b*-PMMA copolymer, the whole system tended to be more miscible like pure PS or PMMA, depending on what component being doped.

(3) On the contrary, the systems with 67% PS-*b*-PMMA copolymer tended to behave as pure PS-*b*-PMMA copolymer owing to its high amount of PS-*b*-PMMA copolymer. The data in the second row of Table I are the *R* values of PS-*b*-PMMA copolymer doped with PS. Among those values, the pair $R_{B12A6B12}$ and R_{B6A3B6} were higher than other pairs with $R_{B12A6B12} > R_{B6A3B6}$ and they are in the first place, $R_{A3B6A3} > R_{A6B12A6}$ and $R_{A3B6} > R_{A6B12}$. Accordingly, the data in the third row of Table I are the *R* values of PS-*b*-PMMA copolymer doped with PMMA. The pair $R_{A6B12A6}$ and R_{A3B6A3} were the highest among all the vales with $R_{A6B12A6} > R_{A3B6A3}$, $R_{B6A3B6} > R_{B12A6B12}$, and $R_{A3B6} > R_{A6B12}$. Though the orders of *R* values in the second and third row were different, they were cause by the same reason. Taking the system of PS-*b*-PMMA copolymer doped with PS as an example, the cause for this result is that its "B" component would prevent the doped A3 or A6 homopolymer from approaching the "A" group in the middle of B6A3B6 copolymer because of the heterogeneity between "A" and "B" components. In addition, the length of B6A3B6 is half of that of B12A6B12, which made the moving ability of B6A3B6 higher than B12A6B12 in adjusting its position, resulting in an ordered domain or even an ordered phase morphology.

(4) For the systems with 55% PS-*b*-PMMA copolymer and doped with PS, the *P* or *R* values both show the heterogeneity between "A" and "B" components. The highest *P* and *R* values of B12A6B12 doped with A6 were obtained because of nearly the reason same as mentioned earlier that its "B" component would

TABLE I
The *R* Values of the 67% PS-*b*-PMMA Copolymer Systems Doped with Ps and PMMA

X=	A3B6	A6B12	A3B6A3	A6B12A6	B6A3B6	B12A6B12
X+PS	0.8647	0.7070	1.0070	0.7599	1.0720	1.4189
X+PMMA	0.9987	0.5911	1.3177	1.4896	1.1708	0.8177

prevent the doped A6 homopolymer from approaching the "A" group in the middle of B12A6B12 copolymer because of the heterogeneity between "A" and "B" components. In addition, B12A6B12 was a long chain with much room to form an aggregation area of the same component. A6B12A6 doped with B12 showed a result similar to that of B12A6B12 doped with A6 with the same reason as shown in subfigure b2 of Figure 2. The first and second highest *R* values above the reference line were for B12A6B12 doped with A6 and B6A3B6 doped with A3 in subfigure b1 in Figure 2 and the first and second highest *R* values above the reference line were for A6B12A6 doped with B12 and A3B6A3 doped with B6 in subfigure b2 in Figure 2. Furthermore, these four values are all above the reference line, which means such a doping ratio is suitable to forming more ordered phase morphology. These results are attributed to the heterogeneity and the difference in diffusion rate and structural characteristics of components.

PS-*b*-PMMA copolymer doped with nanoparticles

Model

To find out the most important factor influencing phase separation, seven different cases doped with column-shaped nanoparticles were built. Table II lists the simulation cases with the nanoparticle number of each layer (N_p), the radium of each nanoparticle (r_p), the height of each nanoparticle (h_p), the layer number (N_L), and the total number of nanoparticles doped (N_{tp}). Among these cases, the 4-3-4-2 case (with four nanoparticles in each layer, radius of 3 nm, height of 4 nm and layer number of 2) was used as the base. Other cases were derived from it and built in the following manners: adding only one more nanoparticle in the center formed Case 4-3-4-3; increasing the layer number to 4, without change in other settings formed Case 4-3-4-4; doubling the nanoparticle density of every layer formed Case 8-3-4-2; doubling the nanoparticle height formed Case 4-3-8-2; adding one more nanoparticle into the middle of the simulation box to increase the layer number to 3 on the basis of Case 4-3-8-2 formed Case 4-3-8-3; doubling the radium of nanoparticles on the basis of Case 4-3-8-2 formed Case 4-6-8-2. Figure 3 shows these seven types of doped nanoparticles arrangements. The chosen parameters were the same as those in the former mesoscopic simulations with the χ values at 383, 413, and 443 K and a total simulation time of 10 ms for each case. The simulation models were also the PS-*b*-PMMA copolymers: A3B6, A6B12, A3B6A3, A6B12A6, B6A3B6, and B12A6B12. Our main objective in this section was to detect what the most important factor influencing phase separation would be: the size, number, density, or the arrangement of the doped nanoparticles.

Results and discussion

Figure 4 shows *P* values of PS-*b*-PMMA copolymer doped with nanoparticles with various parameters. The ranges of *X* axes of six subfigures in Figure 4 were all set from 0.0014 to 0.0075 to compare these data in different subfigures more clearly. The *P* values of six subfigures at 443 K were arranged in an ascending order. Some features can be seen in Figure 4 as follows.

(1) The change tendency of *P* values in six subfigures at 443 K was the same for all the PS-*b*-PMMA copolymer types. Furthermore, the order of *P* values was: $P_{4682} > P_{8342} > P_{4383} > P_{4344} > P_{4382} > P_{4343} > P_{4342}$, which means a more ordered phase morphology could be obtained by increasing the density, size, and number of doped nanoparticles.
(2) The *P* values in subfigures a2, a4, and a6 were higher than those in subfigures a1, a3, and a5, respectively. The orders of *P* values at 383 and 413 K were not completely the same as that at

TABLE II
The Information of Doped Nanoparticles

Number	System	N_p	r_p (nm)	h_p (nm)	N_L	N_{tp}
1	4-3-4-2	4	3	4	2	8
2	4-3-4-3	4	3	4	3	9
3	4-3-4-4	4	3	4	4	16
4	4-3-8-2	4	3	8	2	8
5	4-3-8-3	4	3	8	3	9
6	4-6-8-2	4	6	8	2	8
7	8-3-4-2	8	3	4	2	16

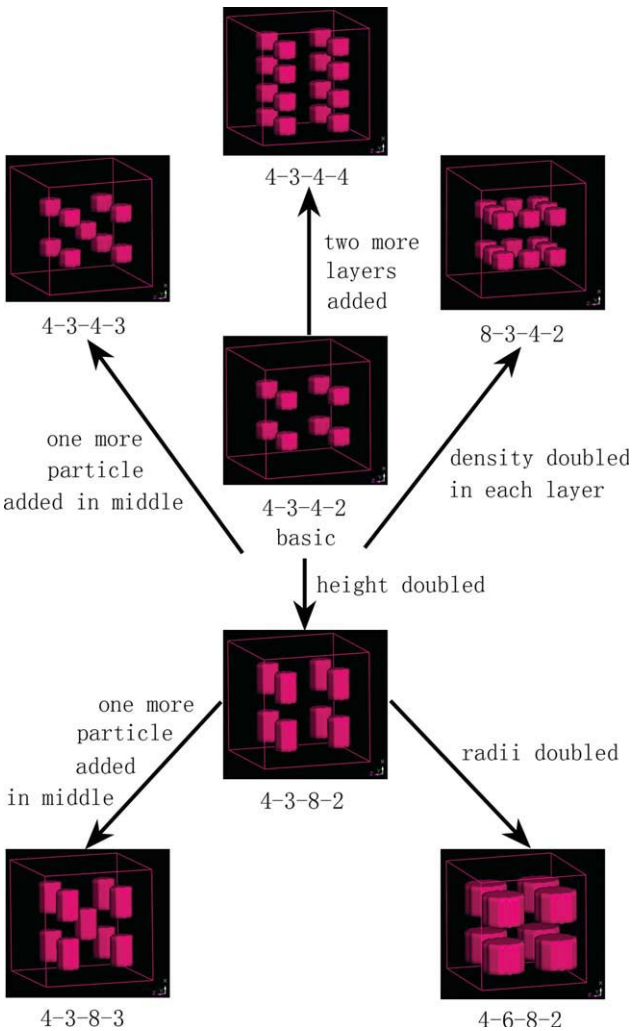

Figure 3 The pictures of seven kinds of nanoparticle arrangement. [Color figure can be viewed in the online issue, which is available at wileyonlinelibrary.com.]

443 K in subfigures a1, a2, a3 and a4, and those cases with P values showing a different order than that at 443 K are named as "defect cases." For example, the P_{4383} value in subfigure a1 was lower than both P_{4344} and P_{8342} values at 383 K and the P_{4344} value in subfigure a2 were higher than both P_{4382} and P_{4383} values at 383 and 413 K; the P_{4383} value in subfigures a3 was lower than both P_{4344} and P_{8342} values at 383 K and P_{4383} and P_{8342} values in subfigure a4 were lower than both P_{4344} and P_{4682} values at 383 and 413 K. The number of "defect cases" (not following the order of P values as it was at 443 K) for long copolymer chains (A6B12 and A6B12A6) was more than the number for short copolymer chains (A3B6 and A3B6A3) accordingly. These results reveal that temperature had a remarkable effect on copolymers with long chains, A6B12, A6B12A6, and B12A6B12, whereas it had hardly any effect on copolymers with short chains, A3B6, A3B6A3, and B6A3B6. This result was contributed by three factors: the heterogeneity between PS and PMMA components in copolymer chain, the chain length, and the difference in diffusion coefficient of PS and PMMA.

(3) On the contrary, the orders of P values were the same at three temperatures in both subfigures a5 and a6 and there was no "defect case" as we mentioned above. Temperature showed almost no effect on such copolymers with long chains, B6A3B6 and B12A6B12, which were composed of more PMMA and both belonged to the "BAB" group.

(4) It can be seen from the difference between the P values under different temperatures for the same kind of PS-*b*-PMMA copolymer, the temperature demonstrated an obvious effect on copolymers with long chains, A6B12, A6B12A6, and B12A6B12 while it showed hardly any effect on their corresponding copolymers with short chains, A3B6, A3B6A3, and B6A3B6. This might result from chain length because the longer the chain the harder for it to move. From an order of $P_{4382} \simeq P_{4344} \simeq P_{4383}$ for copolymers with short chains, it can be seen that the effect of doubling the height of nanoparticles equals to that of doubling the layer number, and it even equals to that of adding one more nanoparticle in the middle of 4-3-8-2 type. This can be explained by the similar nanoparticles' arrangement of 4-3-4-4 and 4-3-8-2 types. The four layers of the 4-3-4-4 type can be divided into two layers with approximate double heights, which was similar to the 4-3-8-2 type. For the 4-3-8-3 type, which had one more nanoparticle in the middle than the 4-3-8-2 type, the effect of adding one more nanoparticles was not obvious on changing its P value especially for PS-*b*-PMMA copolymer doped with high height nanoparticles.

Figure 5 shows the corresponding R values of copolymers doped with nanoparticles in Figure 4. The R values are defined as the quotients of P values of PS-*b*-PMMA copolymer doped with nanoparticles being divided by the P value of the plain PS-*b*-PMMA copolymer. The spans of X axes of the six subfigures in Figure 5 were set from 0.4 to 5.5 for the convenience of comparison of these data from different subfigures. The R values of these six kinds of PS-*b*-PMMA copolymer at 443 K were arranged in an ascending order to make a comparison with Figure 4. There are some features in common between Figures 5 and 4. First, the change tendency of values

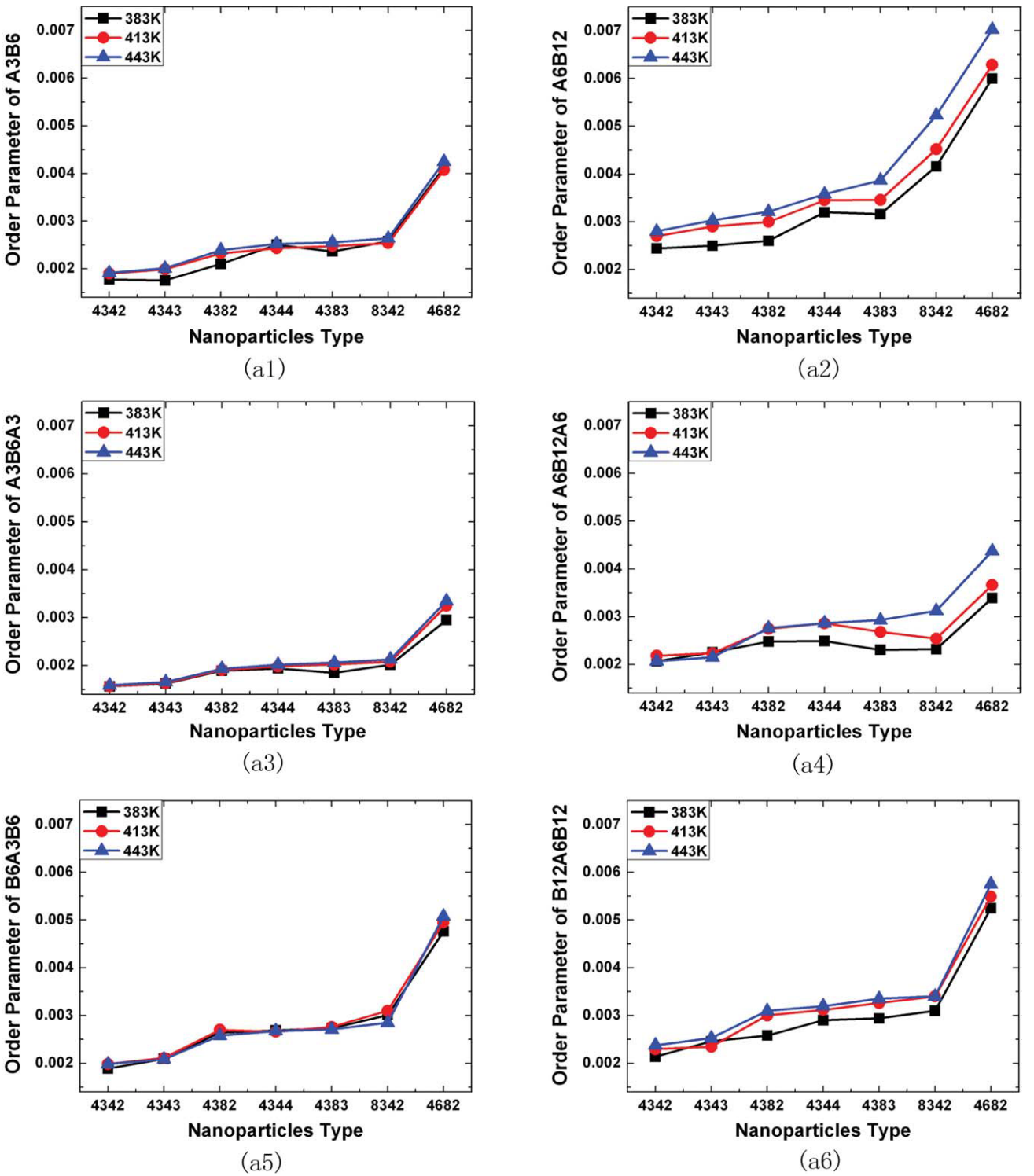

Figure 4 The *P* values of six kinds of PS-*b*-PMMA copolymers doped with nanoparticles at 383, 413, and 443 K, respectively. [Color figure can be viewed in the online issue, which is available at wileyonlinelibrary.com.]

in six subfigures was the same, and the order of *R* values was the same as it in Figure 4, which was, $R_{4682} > R_{8342} > R_{4383} > R_{4344} > R_{4382} > R_{4343} > R_{4342}$. Second, the "defect cases" in subfigures b1, b2, b3, and b4 were the same as those in subfigures a1, a2, a3, and a4 of Figure 4, respectively. Third, there was no "defect case" in subfigures b5 and b6, which is the same as that in subfigures a5 and a6 of Figure 4. Fourth, from the difference between the *R* values under different temperatures for the same kind of PS-*b*-PMMA copolymer, it can be seen that temperature showed an obvious effect on

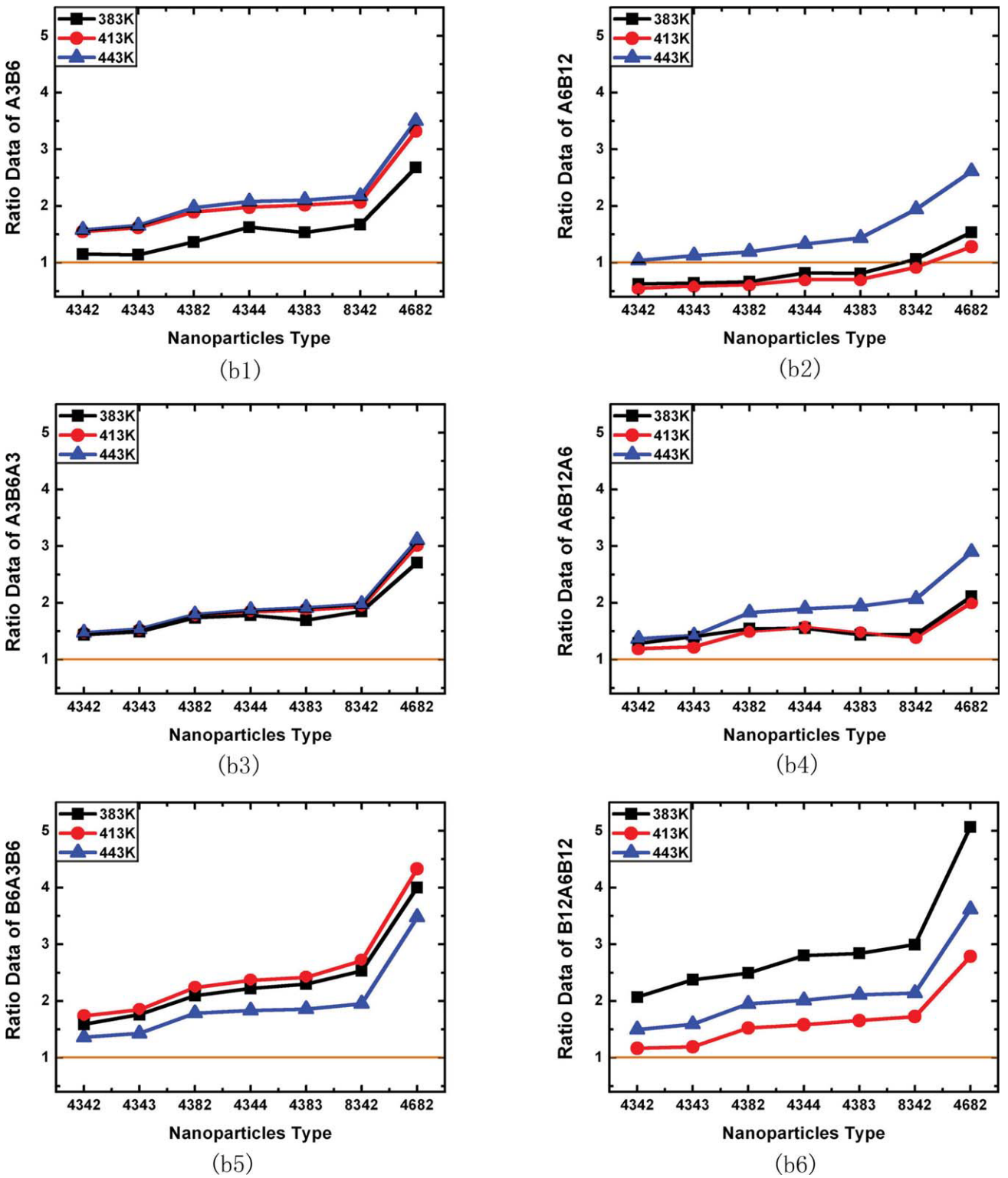

Figure 5 The *R* values of six kinds of PS-*b*-PMMA copolymers doped with nanoparticles at 383, 413, and 443 K, respectively. These data are originated from Figure 4. [Color figure can be viewed in the online issue, which is available at wileyonlinelibrary.com.]

copolymers with long chains, A6B12, A6B12A6, and B12A6B12, which was different from its effect on the corresponding copolymers with short chains, A3B6, A3B6A3, and B6A3B6. However, there is a unique feature in Figure 5. The *R* values are all above the reference line except that for the A6B12 copolymer. In subfigure b2, the following *R* values are above the reference line: all *R* values at 443 K, the *R* values

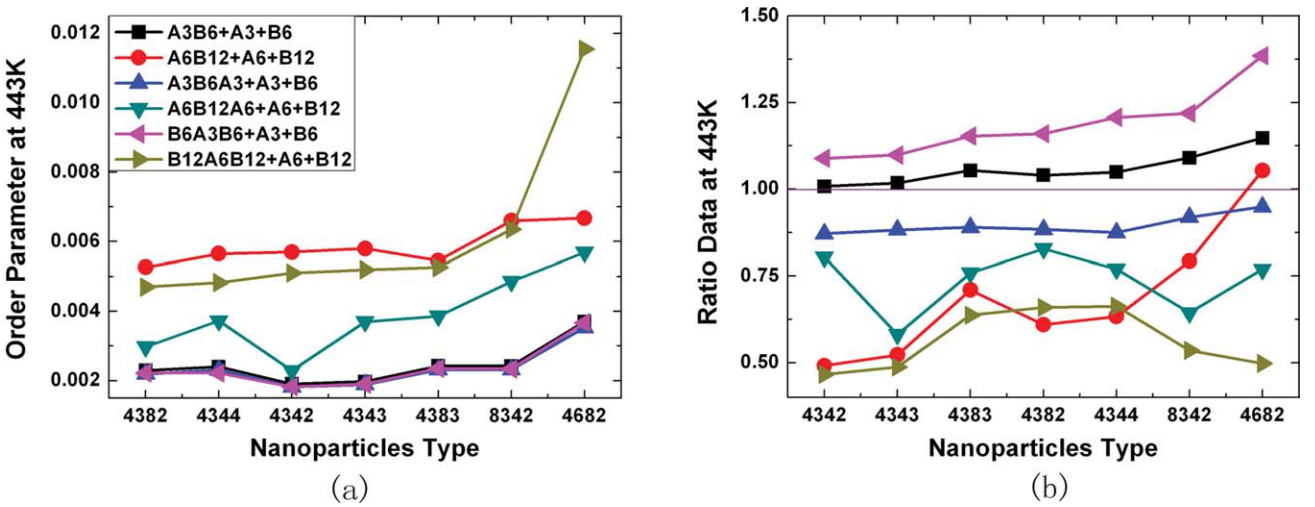

Figure 6 The *P* and *R* values of six kinds of PS-*b*-PMMA copolymers doped with both PS and PMMA and seven types of nanoparticle arrangement at 443 K. The *R* values were based on plain PS-*b*-PMMA copolymer doped with nanoparticles. [Color figure can be viewed in the online issue, which is available at wileyonlinelibrary.com.]

of PS-*b*-PMMA copolymer doped with 4-6-8-2 and 8-3-4-2 nanoparticles at 383 K, and the *R* values of PS-*b*-PMMA copolymer doped with 4-6-8-2 nanoparticles at 413 K. On the contrary, the other *R* values are below the reference line, which means that doping nanoparticles had a weakening effect on changing the phase morphology of the PS-*b*-PMMA copolymer.

PS-*b*-PMMA copolymer doped with its own constructing components

Model

The models of this part were all constructed with three components, PS-*b*-PMMA copolymer, PS, and PMMA with weight percentages of 18, 41, and 67%, respectively. The simulation temperature was 443 K to make a comparison with the cases in Figure 2. Such three components were related with each other in a way that the doped copolymers were made up with both PS and PMMA components with the same chain lengths as their corresponding homopolymers. These six kinds of models included A3B6 doped with A3 and B6, A6B12 doped with A6 and B12, A3B6A3 doped with A3 and B6, A6B12A6 doped with A6 and B12, B6A3B6 doped with A3 and B6, and B12A6B12 doped with A6 and B12.

Results and discussion

Figure 6 shows the *P* and *R* values of the six models above. The following features are seen in the figure.

(1) In subfigure a, an unusual case is shown, which was the B12A6B12 copolymer doped with both A6 and B12 homopolymers and 4-6-8-2 nanoparticles. The *P* value of this case was the highest among all the cases. For other cases, no matter what kinds of nanoparticles were doped, the order of *P* values was $P_{\mathrm{A6B12+A6+B12}} > P_{\mathrm{B12A6B12+A6+B12}} > P_{\mathrm{A6B12A6+A6+B12}} > P_{\mathrm{A3B6+A3+B6}} \simeq P_{\mathrm{A3B6A3+A3+B6}} \simeq P_{\mathrm{B6A3B6+A3+B6}}$. From this relationship, it can be seen that the *P* values are dependent on the length of copolymers and homopolymers.

(2) For long chain systems, the orders of their *P* values were the same as the plain copolymers, which was $P_{\text{“AB”}} > P_{\text{“BAB”}} > P_{\text{“ABA”}}$, but the *P* values of those with nanoparticles doped were much higher than the *P* values in plain copolymers. In addition, for short chain systems, their *P* values were also higher than the plain copolymers, except for the system of A6B12 doped with A6 and B12.

(3) In subfigure b, the *R* values were obtained based on the *P* values of plain copolymers doped with the corresponding kinds of nanoparticles at 443 K in shown Figure 4. The *R* value of B6A3B6 doped with A3 and B6 was the highest compared with the other systems doped with the same nanoparticles with the same arrangement, which means this system suffered the most from doping of the homopolymer in regard to its phase morphology. In addition, the *R* value of A3B6 copolymer doped with A3 and B6 was the second highest. Furthermore, the R values of these two systems are all above the reference line, which means doping with these homopolymers for such B6A3B6 and A3B6 copolymers promoted changes of their phase morphologies. On the contrary, the others cases showed weakening effects.

The PS/PMMA blends were immiscible. In addition, the R values in Figure 5 at 443 K are all above the reference line, but only two systems doped with two homopolymers showed more orderly phase morphologies in subfigure b of Figure 6. This resulted from the copolymer structure and the difference in diffusion coefficient between PS and PMMA. B6A3B6 and A3B6 both belonged to short chain systems, and their weight percentages of "B" component were all higher than A3B6A3 copolymer. The short chains are more flexible in movement than the longer ones, so it would response more violently to the changes in the external environment, adjusting its configuration to form domains with same components and even undergoing phase separation.

CONCLUSIONS

Six kinds of block copolymers could be classified into three types according to the characteristics in copolymer structures, "AB", "BAB" and "ABA", and the order of their P values was $P_{\text{"AB"}} > P_{\text{"BAB"}} > P_{\text{"ABA"}}$. The P values of long chains were all higher than their corresponding short ones. These plain copolymers doped with the PS or the PMMA homopolymer showed different P values with certain weight percentages of PS-*b*-PMMA copolymer; the triblock copolymer composed of the same component at both ends and doped with the homopolymer with the same component as the middle component in the triblock copolymer showed the highest R values; these cases included B6A3B6 doped with A3, B12A6B12 doped with A6, A6B12A6 doped with B12, and A3B6A3 doped with B6.

Mesoscopic simulations were carried out on the plain PS-*b*-PMMA copolymers doped with nanoparticles with various sizes, densities, and arrangements. The simulation results show that doping with nanoparticles is a good way of improving the degree of order of the mesoscopic phases. The order of P value was $P_{4682} > P_{8342} > P_{4383} > P_{4344} > P_{4382} > P_{4343} > P_{4342}$ at 443 K and the order of R values was the same for these simulations. Furthermore, their R values are all above the reference line, which means more orderly phase morphology, could be obtained by increasing the density, size and number of doped nanoparticles. Among them increasing the size of doped nanoparticles was the most efficient method. However, for A6B12 copolymer, doping nanoparticles was only efficient for 4-6-8-2 and 8-3-4-2 at 383 and 413 K, which can be seen from their R values being above the reference line.

When the copolymers are doped with PS and PMMA homopolymers, though the P values of doping with 4-6-8-2 nanoparticles were the highest, only the B6A3B6 and A3B6 doped with their corresponding homopolymers show a reinforcing effect on changing the phase morphologies while all the other cases showed a weakening effect.

References

1. Guarini, K. W.; Black, C. T.; Milkove, K. R.; Sandstrom, R. L. J Vac Sci Technol B 2001, 19, 2784.
2. Asakawa, K.; Hiraoka, T.; Hieda, H.; Sakurai, M.; Kamata, Y.; Naito, K. Japan J Appl Phys 2002, 41, 6112.
3. Mansky, P.; Chaikin, P.; Thomas, E. L. J Mater Sci 1995, 30, 1987.
4. Mansky, P.; Harrison, C. K.; Chaikin, P. M.; Register, R. A.; Yao, N. Appl Phys Lett 1996, 68, 2586.
5. Park, M.; Harrison, C. K.; Chaikin, P. M.; Register, R. A.; Adamson, D. H. Science 1997, 276, 1401.
6. Herrninghaus, S.; Jacobs, K.; Mecke, K.; Bischof, J.; Fery, A.; Ibn-Elfraj, M.; Schlagowski, S. Science 1998, 282, 916.
7. Averopoulos, A.; Chan, V. Z.-H.; Lee, V. Y.; No, D.; Miller, R. D.; Hadjichristidis, N.; Thomas, N. L. Chem Mater 1998, 10, 2109.
8. Thurn-Albrecht, T.; Schotter, J.; Kästle, A.; Emley, N.; Shibauchi, T.; Krusin-Elbaum, L.; Guarini, K.; Black, C. T.; Tuominen, M. T.; Russell, T. P. Science 2000, 290, 2126.
9. Thurn-Albrecht, T.; Steiner, R.; Derouchey, J.; Stafford, C. M.; Huang, E.; Ball, M.; Tuominen, M.; Hawker, C. J.; Russell, T. P. Adv Mater 2000, 12, 787.
10. Black, C. T.; Guarini, K. W.; Milkove, K. R.; Baker, S. M.; Tuominen, M. T.; Russell, T. P. Appl Phys Lett 2001, 79, 409.
11. Paul, D. R.; Newman, S. Polymer Blends; Academic Press: New York, 1978.
12. Abd-El-Messieh, S. L. Polym Plast Technol Eng 2003, 42, 153.
13. Schneider, I. A.; Calugaru, E. M. Eur Polym J 1976, 12, 879.
14. Bada, R.; Perez Jubindo, M. A.; De, L. A.; Fuente, M. R. Mater Chem Phys 1987, 18, 359.
15. Zhu, P. P. Eur Polym J 1997, 33, 411.
16. Lee, J. K.; Han, C. D. Polymer 1999, 40, 6277.
17. Lee, C. F. Polymer 2000, 41, 1337.
18. Li, X.; Han, Y.-C.; An, L.-J. Polymer 2003, 44, 8155.
19. Walheim, S.; Boltau, M.; Mlynek, J.; Krausch, G.; Steiner, U. Macromolecules 1997, 30, 4995.
20. Schmidt, J. J.; Gardella, J. A.; Salvati, L. Macromolecules 1989, 22, 4489.
21. Chiou, J. S.; Barlow, J. W.; Paul, D. R. J Polym Sci Part B: Polym Phys 1987, 25, 1459.
22. Lhoest, J. B.; Bertrand, P.; Weng, L. T.; Dewez, J. L. Macromolecules 1995, 28, 4631.
23. Davies, M. C.; Shakesheff, K. M.; Shard, A.; Domb, A.; Roberts, C. J.; Tendler, S. J. B.; Williams, P. M. Macromolecules 2000, 29, 2205.
24. Valls, O. T.; Farrell, J. E. Phys Rev E 1993, 47, R36.
25. Ramirez-Piscina, L.; Hernández-Machado, A.; Sancho, J. M. Phys Rev B 1993, 48, 125.
26. Kawakatsu, T.; Kawasaki, K.; Furusaka, M.; Okabayashi, H.; Kanaya, T. J Chem Phys 1993, 99, 8200.
27. Shinozaki, A.; Oono, Y. Phys Rev E 1993, 48, 2622.
28. Mu, D.; Huang, X.-R.; Lu, Z.-Y.; Sun, C.-C. Chem Phys 2008, 348, 122.
29. Mark, J. E. Polymer Data Handbook; Oxford University Press, Inc.: New York, 1999.